Research Article

Received: 11 October 2010 Revised: 3 March 2011 Accepted: 22 March 2011 Published online in Wiley Online Library: 26 April 2011

(wileyonlinelibrary.com) DOI 10.1002/jctb.2638

Modelling diffusion and adsorption of As species in Fe/GAC adsorbent beds

Mirna E. Sigrist,[a] Horacio R. Beldomenico,[a] Enrique E. Tarifa,[b] Carlos L. Pieck[c] and Carlos R. Vera[c]*

Abstract

BACKGROUND: Arsenic decontamination of drinking water by adsorption is a simple and robust operation. When designing packed bed adsorbers for arsenic, the main problems are the slow diffusion kinetics of As in microporous media and the lack of simple equations for predicting the performance of the equipment. Commercial iron-doped granular activated carbon adsorbents (Fe/GAC) for groundwater arsenic abatement were studied in this work. Basic parameters for arsenate (As^V) adsorption were measured and their performance at larger scale was simulated with an approximate analytical model.

RESULTS: In the 0–300 $\mu g_{As}\ L^{-1}$ range, the As^V adsorption isotherm on Fe/GAC was found to be approximately linear. Assuming Henry's law for adsorption and homogeneous surface diffusion with constant diffusivity for intrapellet mass transfer, an approximate model for flow and adsorption of arsenate inside packed bed adsorbers was developed, and reduced to an analytic compact solution using the quasi-lognormal distribution (Q-LND) approximation. The use of this model with fitted and reported parameters enabled the approximate simulation of industrial adsorbers and home point-of-use filters. Results show that industrial adsorbers meet the breakthrough condition with incomplete utilization of the adsorbent unless convenient process configurations are used. In point-of-use systems with short residence times intraparticle diffusion would drastically reduce the adsorbent performance.

CONCLUSION: Assuming linear adsorption of As^V over Fe/GAC, an analytical approximate solution for flow and adsorption in packed beds can be obtained. The model seems to represent correctly the main features of industrial and home filters, however, more experimental data is necessary for scale-up purposes.

Keywords: iron; GAC; adsorption; arsenic abatement

INTRODUCTION

Arsenic in groundwaters has received a lot of attention from environmental agencies, researchers and the public because of the noxious effect of arsenic on human health and on biota. In most countries the arsenic level in drinking water is limited to a maximum of 50 $\mu g\ L^{-1}$ but in the more developed countries, in recent years the limit has been reduced to 10 $\mu g\ L^{-1}$.[1]

The Chaco-Pampean Plain of central Argentina is one of the largest regions of high arsenic (As) groundwaters known, covering one million square kilometers. These high-As groundwaters (up to 5000 $\mu g\ L^{-1}$) are from Quaternary deposits of loess (mainly silt) with intermixed rhyolitic or dacitic volcanic ash.[2] The groundwaters of the region are oxidizing, with dissolved oxygen, nitrate and sulfate. For this reason As^V is the dominant dissolved species with As^{III}/As^{total} ratios as low as 0.02–0.06[3] or with negligible As^{III} content.[4] The objects of this study are adsorbents for As abatement in this area and therefore attention is focused on the main pollutant, As^V.

Many arsenic abatement techniques have been proposed but those most often used are flocculation, reverse osmosis and adsorption.[5] Flocculation needs rather large installations, trained personnel and consumes a relatively large amount of chemicals per unit mass of arsenic removed. Reverse osmosis (RO) has high efficiency (up to 86% As rejection[6]) and is especially recommended for groundwaters with a high content of dissolved solids. However, the cost of installation and maintenance of RO plants is high. The capital cost of a plant is 1.24 USD per gallon per day of product water installed[7] while the cost of a household point-of-use system can be 1000 USD.[6] So the preferred method for point-of-use (drinking tap) arsenic removal is adsorption because of the simplicity of operation and the relatively low cost of installation. However, the use of adsorbents in industrial plants is not widespread but the high efficiency of As removal and the relatively low cost of implementation has resulted in adsorption being labelled the 'best available technique' (BAT) for arsenic removal, by the US EPA.[8]

* *Correspondence to: Carlos R. Vera, INCAPE, Santiago del Estero 2654, 3000 Santa Fe, Argentina. E-mail: cvera@fiq.unl.edu.ar*

a *Laboratorio Central de la Facultad de Ingeniería Química, Universidad Nacional del Litoral, Santiago del Estero 2654, 3000 Santa Fe, Argentina*

b *Facultad de Ingenieria, Universidad Nacional de Jujuy, Gorriti 237, 4600 San Salvador de Jujuy, Argentina*

c *Instituto de Investigaciones en Catálisis y Petroquímica, INCAPE (FIQ-UNL, CONICET), Santiago del Estero 2654, 3000 Santa Fe, Argentina*

Adsorbents for the removal of arsenic are almost invariably based on bulk or supported particles of transition metal oxides and hydroxides. Supported adsorbents are composed of a porous 'support' or 'carrier' with appropriate textural properties (specific surface area, porosity, average pore radius, mechanical strength, etc.), and usually consist of activated carbon, alumina or silica, and an active phase with an affinity for the adsorbate that is 'supported' or 'dispersed' over the carrier. Such a combination of materials is useful when it is difficult to provide a bulk active phase with convenient textural properties.

The preferred transition metals used in adsorbents are Fe, Zr and Ti. Fe is commonly used in high throughput applications because of the low cost of fabrication of the adsorbent. Thus the convenience of using Fe minerals in packed columns as a means of removing arsenic has been well studied.[9,10] In the case of granular ferric hydroxide (GFH) and arsenate, it has been found that proportional diffusivity scaling is the most appropriate[10] and different derivations of the homogeneous surface diffusion model have been proposed.[9] Reviews[11] indicate that the adsorption capacity of GFH is in the range of 1000–30 000 bed volumes for an outlet breakthrough As concentration of 10 $\mu g\ L^{-1}$.

The adsorption capacity of an iron-based filter is highly dependent on the number of exposed iron species and therefore industrial adsorbents are specially fabricated to maximize the specific surface area of the iron particles. Such high surface areas are commonly obtained by reducing the size of bulk iron oxide particles to the nanoparticulate range.[12,13] Another strategy is that of supporting iron species on a support of high specific surface area, such as alumina, activated carbon or resins.[14,15] In general bulk catalysts have a higher adsorption capacity per unit volume of filter. However, supported adsorbents are sometimes preferred for use in packed beds because of their much lower cost and optimized textural properties.

Commercial adsorbents based on iron supported on activated carbon have a convenient combination of properties: good arsenic adsorption capacity; low cost and additional capacity for adsorption of chlorine, organic compounds, odorants, heavy metals and bacteria.[16,17] Commercial Fe/GAC adsorbents with 10% Fe loading were studied in this work. Their adsorption capacity for As^V was measured experimentally by both equilibrium adsorption and column breakthrough tests. An approximate analytical model was then used to simulate the performance of Fe/GAC packed bed adsorbers and assess the best parameters for their design and operation.

EXPERIMENTAL

Materials

An iron impregnated granular activated carbon (BPV s.r.l., Sauce Viejo, Argentina) was used in the experimental work. The adsorbent was supplied in 12 × 40 granules and contained 10% w/w Fe. The supplier indicated that the main iron species in the adsorbent was hydrated ferric hydroxide. Smaller adsorbent particle sizes were obtained by crushing and screening. The adsorbent was pretreated by drying at 110 °C for 1 day and then it was kept in a desiccator for further use. A solution of arsenic was prepared from deionized water and sodium arsenate (Sigma-Aldrich, CAS 10 048-95-0, >98%). The As content of the solutions was determined by atomic absorption as follows.

Arsine method

An on-line system based on flow injection hydride generation atomic absorption spectrometry (FI-HGAAS) with a heated quartz tube atomizer was used for the determination of As. HGAAS is a very widely used technique for the ultratrace determination of arsenic, selenium, bismuth and other elements able to generate volatile hydrides. This technique involves the reaction of arsenic in a reducing and acid media to produce arsine (AsH3), allowing an increase of sensitivity and selectivity of the analytical determination in comparison with conventional AAS. Flow injection (FI) is particularly advantageous in making the hydride generation easier. A Perkin-Elmer Model 3110 flame atomic absorption spectrometer was used as detector. It was equipped with a Photron arsenic hollow cathode lamp set at 193.7 nm wavelength, 11 mA lamp current and 0.7 nm slit width. A Perkin-Elmer FIAS 100 flow injection hydride generation system with a heated quartz tube atomizer (10 mm i.d. × 160 mm length) was used for hydride generation.

Equilibrium data

The equilibrium isotherm was determined at 25 °C over a range of arsenic concentrations in the fluid phase from 0.1 to 20 000 $\mu g\ L^{-1}$. After adding the corresponding sodium arsenate aliquot the solution was stabilized to a target pH value of 7.5 ± 0.3 with $NaHCO_3$. No other salts were used in the solution. Additional $NaHCO_3$ was added dropwise to keep the pH at a stable value during adsorption. The solid–liquid mixtures were allowed to equilibrate for 1 day with periodic gentle stirring. The time of equilibration was taken from reports on the adsorption of arsenic on Fe/GAC adsorbents.[14,15] Each point corresponds to a duplicate measurement; in a few cases the error was large and a third test was performed for checking. The concentration in the adsorbed phase was found by a mass balance from the initial and final concentrations in the fluid. In a typical adsorption experiment the adsorbent (2 g) was crushed and sieved to 100 mesh and immersed in a solution (100 mL) of known As composition. The solution was left at room temperature with periodic gentle stirring (10 min every 2 h). The pH was adjusted to the desired value by $NaHCO_3$ addition. After 24 h stirring was stopped and the suspended solids were allowed to settle by gravity. Samples (2 mL) were taken from the bulk liquid phase and analyzed by atomic absorption as above.

Fixed-bed breakthrough curves (rapid small scale column tests, RSSCT)

Breakthrough experiments were carried out in stainless steel columns (9 mm diameter, 30 cm height) packed with adsorbent (25 cm long, 35–80 mesh particle size). The column was maintained at 25 °C, and the feed, an arsenic solution containing 100 ppb As^V was introduced from the top at 18.5 mL min^{-1} by a positive displacement pump (Dosivac 2070). The downflow arrangement was adopted to prevent expansion of the bed and subsequent channeling of the fluid stream. Samples of the effluent from the column were collected at suitable time intervals and analyzed by the arsine method. The curves were measured only once, i.e. no duplicate tests were performed.

Simulation

All numerical analysis was performed with the aid of MatLab for Windows R2010a software. The adjustment of the model parameters was carried out using a Levenberg–Marquardt algorithm for least-squares minimization of the deviation between the experimental and theoretical data.

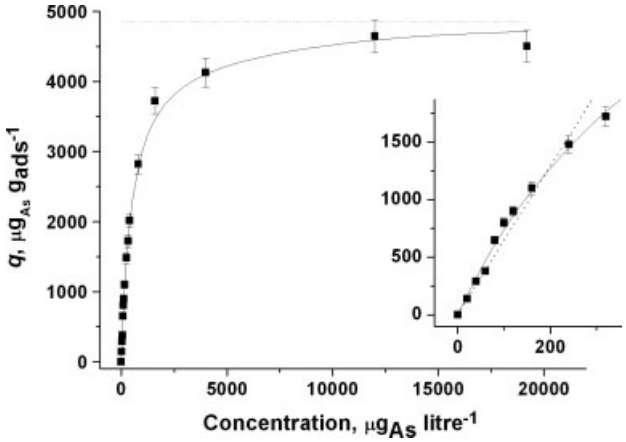

Figure 1. Equilibrium isotherm for As^V. (■) Experimental points. Dotted line: square isotherm approximation. Langmuir parameters: $K = 1.8\ \mu g_{As}^{-1}\ L$, $q_m = 4850\ \mu g_{As}\ g_{ads}^{-1}$. Inset: high dilution range. Henry's law parameter: $H = 8.51\ L\ g_{ads}^{-1}$.

RESULTS AND DISCUSSION

Arsenate equilibrium adsorption tests

Results of the arsenate equilibrium adsorption tests are shown in Fig. 1. The error of the As titration method was found to be 0.8–1.7 µg L^{-1}, while the overall repeatability of the isotherm points was about 5% of the average (indicated as error bars in Fig. 1). When plotting the full range As^V adsorption isotherm it can be seen that the data can be fitted well by a classical Langmuir isotherm. Three concentration ranges can be distinguished. Thus for As^V concentrations higher than 5000 $\mu g_{As}\ L^{-1}$ the adsorbate becomes saturated and the concentration is equal to the maximum adsorption capacity, q_m, i.e. 1850 $\mu g_{As}\ g_{ads}^{-1}$. For As^V concentrations less than 2000 $\mu g_{As}\ L^{-1}$ the adsorption equilibrium can seemingly be described by a Freundlich isotherm, and for even more dilute solutions, e.g. 0–300 $\mu g_{As}\ L^{-1}$ a linear isotherm can be adopted. In this case adsorption fitted Henry's law with $H = 3.5\ g_{ads}^{-1}\ L$. It can be seen that for concentrated solutions the square isotherm approximation is valid ($q = q_m$), while for diluted solutions a linear aproximation is appropriate ($q = HC_{As}$). The linear isotherm model for the arsenic–Fe/GAC system is valid for the range 0–300 $\mu g_{As}\ L^{-1}$. Over the full range of concentrations the Langmuir formula can be used (Equation (1)), with $K = 0.0018\ \mu g_{As}^{-1}\ L$.

$$q = \frac{q_m K_L C}{1 + K_L C} \tag{1}$$

The uncertainty in the adsorption parameters H, K and q_m depends largely on the time scale of the experiment and the size of particles used. One unforeseen detail is that owing to the extremely small surface diffusivity of the arsenate ion the time taken to attain complete equilibrium can be several days or weeks. For example Badruzzaman[11] indicated that after 18 days arsenate adsorption equilibrium was not achieved in 30 × 60 and 10 × 30 granular ferric hydroxide (GFH) particles. Therefore the values of H, K and q_m obtained should be considered as minimum values. As the diffusion flux is proportional to the concentration gradient, equilibrium should be more rapidly attained in highly concentrated solutions while equilibrium should be very slow in the high dilution range. For this reason q_m values should have a low uncertainty while H could be prone to underestimation. This is evident when analyzing some data found in the literature on arsenate adsorption over highly microporous adsorbents, for example the data for As^V adsorption over Fe/GAC adsorbents obtained by Gu *et al.*[14] and Chen *et al.*[15] where both equilibrium adsorption tests and RSSCTs were performed. Equilibrium adsorption tests covered 24 h while RSSCTs could be as long as 50–70 days. The data for these tests are summarized in Table 1 and are compared with those obtained with a Fe/C adsorbent with mesoporous structure.[12]

We can define the nominal adsorption capacity (Q^*) as the maximum amount of water (volume) that can be treated per unit mass of adsorbent, considering that the solid is fully saturated. This value is a function of the feed concentration C^o and in the case of the equilibrium adsorption test it would be the amount of arsenate adsorbed in infinite contact time. In the case of the breakthrough tests this value would be the breakthrough value at an infinitely slow rate of elution. The following equalities can be derived for the linear isotherm model (Equation (2)), the square isotherm model (Equation (3)) and the experimental RSSCT (Equation (4)).

$$Q^* = H \tag{2}$$

$$Q^* = \frac{q_m}{C^o} \tag{3}$$

$$Q^* = \frac{\int_0^\infty (C^o - C)dV}{C^o W_{ads}} \tag{4}$$

When the values of Q^* in Table 1 for references 14 and 15 are examined it can be seen that the experimental values from the RSSCT are always much smaller than those predicted by the square isotherm model, and larger than those predicted by the linear model. The equilibrium adsorption isotherms plotted in references 14 and 15 clearly indicate that under the conditions of the RSSCTs, the relation between q and arsenic concentration is linear. Therefore the underestimation of Q^* by the linear model must be due to underestimation of the H constant. This is probably a problem of the time scale of the static adsorption experiment.

Table 1. Adsorption equilibrium parameters (As^V) and total adsorption capacity (as calculated from breakthrough curves) for different Fe/GAC adsorbents

				Q^*, $m^3\ kg_{ads}^{-1}$			
Fe, %	H, $L\ g_{ads}^{-1}$	q_m, $\mu g_{As}\ mg_{ads}^{-1}$	C^o, $\mu g_{As}\ L^{-1}$	Experimental	Linear isotherm model	Square isotherm model	Ref.
5.8	5.0–10.0	3.8	57.2	18.0	7.5	66.4	6
11.7	7.5–8.8	43.6–51.3	40.0	38.0	8.15	1200	7
3.85	≈40[(1)]	6.46	–	–	–	–	12

[1] Calculated from $q_m * K$ (for C_{As} infinitely small in Langmuir's formula).

To sidestep this problem the time for equilibrium should be made equal to the time span of the RSSCT. Another solution is to obtain H with the aid of a breakthrough curve from a RSCCT and the use of Equations (2) and (4). This approach will be used in the following sections. It can also be seen in Table 1 that higher values of H (and hence of K) have been measured in mesoporous Fe/C.[18] This is in agreement with the hypotheses of long diffusion times in microporous systems and much shorter times in mesoporous systems.

With respect to the use of a linear isotherm or a Freundlich isotherm, our results and those reported in references 14, 15 and 18, can be fitted reasonably well by a straight line in the 0–300 $\mu g_{As}{}^{-1}$ L range. In other reports, however, this is not the case. Thus the data of Sperlich *et al*.[9] for the adsorption of arsenate on granular ferric hydroxide (GFH) seem to be better fitted by a Freundlich isotherm, and the q–C curve is approximately linear only over the 0–100 $\mu g_{As}{}^{-1}$ L range. The data reported by Hristovski *et al*.[19] for the adsorption of As on Fe/GAC are highly non-linear and seem to be fitted reasonably well only by the Freundlich isotherm, even in the high dilution range.

Derivation of fixed bed adsorption theoretical breakthrough curves

At this point it must be said that *approximate* analytical breakthrough curves will be derived in order to obtain *approximate* relations between the variables and to capture the main features of the system. However, the main purpose is not to provide tools for an accurate scale-up of Fe/GAC industrial adsorbers. This task would require much more experimental evidence, especially in the form of breakthrough curves for industrial units.

To model the adsorption of arsenic over the adsorbent bed several simplifying assumptions were made. (i) The whole system was considered to be isothermal. This is strictly true because arsenate is highly diluted and the ratio of the heat of reaction to the thermal capacity of the fluid is practically negligible. (ii) The flow pattern was assumed to be axially dispersed Fickian flow and radial concentration gradients in the adsorption bed were considered negligible. (iii) The axial diffusion D_L and the film coefficient k_f were assumed to obey the Wakao and Funazkri correlations (Equations (6) and (7)), that have been demonstrated to reliably represent particle-to-fluid mass transfer in systems of porous particles immersed in gas or liquid streams.[20] (iv) Transfer through the film of the pellet was described by a classical linear relation (Equation (8)). (v) Adsorption inside the pellet was assumed to follow a general Langmuir isotherm (Equation (1)) as proposed for the Fe/GAC system elsewhere.[15]

With respect to hypothesis (ii), axial dispersion contributes to the broadening of the adsorption front and comes from the contribution of both molecular diffusion and dispersion caused by fluid flow.[20] In the case of the As^V–(Fe/GAC) system only the second is important, as can be seen by inspecting the reported value of the molecular diffusivity (Ouvrard *et al*.[21]) and calculating with the Wakao and Funazkri equation.[20] The impact of the axial dispersion is assessed by the Péclet number (Pe), small values indicating dispersion is important for mass transfer. According to Carberry[22] for Pe values much greater than 100 the flow can be considered plug-flow type. For simulations of an industrial adsorber in this work, Pe = 200–1500, while for the small column tests Pe > 1000. According to this axial dispersion is negligible in most cases but could be important in a few. For this reason axial backmixing was taken into account.

In the case of the radial concentration pattern, the magnitude of the gradient in fixed bed adsorbers depends on the non-linearity of the adsorption isotherm and the magnitude of the non-plug-flow-velocity profile.[23] A plug flow inlet velocity profile was assumed and radial gradients were therefore disregarded.

Applying these assumptions to a mass balance through a packed bed, Equations (5)–(13) were obtained where D_L is the axial dispersion coefficient, C is the concentration in the fluid phase, u denotes superficial velocity, q_{av} is the volume-averaged adsorbed concentration, ε denotes the total bed porosity, hence $(1-\varepsilon)$ denotes the fractional volume taken up by the solid phase, z is the axial distance from column entrance, r is the radial coordinate, R_p is the radius of the adsorbent and ρ_S is the density of the adsorbent.

$$\frac{\partial C}{\partial t} - D_L\frac{\partial^2 C}{\partial z^2} + \frac{\partial (uC)}{\partial z} + \frac{1-\varepsilon}{\varepsilon}\rho_s\frac{\partial q_{av}}{\partial t} = 0 \tag{5}$$

$$\frac{D_L}{2uR_p} = \frac{20}{\mathrm{Re}\,Sc} + 0.5 \tag{6}$$

$$k_f = (2.0 + 1.1Sc^{1/3}\mathrm{Re}^{0.6})\frac{D_m}{2R_p} \tag{7}$$

$$\frac{\partial q_{av}}{\partial t} = (3k_f/(R_p\rho_s))(C - C_s) \tag{8}$$

$$C(0,t) = C^0 \tag{9}$$

$$\frac{\partial C}{\partial z} = 0,\ z = L \tag{10}$$

$$C(z,0) = 0 \tag{11}$$

$$\frac{\partial q}{\partial t} = D_s\left(\frac{\partial^2 q}{\partial r^2} + \frac{2}{r}\frac{\partial q}{\partial r}\right) \tag{12}$$

$$q_{av} = (3/R_p^3)\int_0^{Rp} r^2 q\, dr \tag{13}$$

A further explanation of the meaning of each symbol is given in Table 2 along with estimates taken from the scientific literature. Equations (9)–(11) are the 'clean bed' initial condition and the Danckwertz boundary conditions for a closed system. Equation (12) is the equation for Fickian diffusion inside the pellet, where q is the adsorbed concentration in the adsorbent shell, D_S is the surface diffusivity, r is the radial distance in the adsorbent particles. Equation (13) is the expression for the average adsorbed concentration, q_{av} with C_s the arsenate concentration at $r = R_p$. Since inside the pellet and on its surface the adsorption is supposed to be in equilibrium, $q_s = q(C_s)$.

Equations (8) and (12) are those of the so-called homogeneous surface diffusion model (HSDM). In this model the adsorbent is supposed to be a homogeneous solid sphere in which the adsorbate is transported by surface diffusion. The rate controlling steps are mass transport based on the film (Equation (8)) and surface diffusion (Equation (12)) models only. A driving force describes the liquid film transport resistance at the external surface of the particle. The HSDM model has been used previously to model adsorption of arsenic in Fe/GAC pellets.[24]

In Equation (12) a constant value of diffusivity was adopted. In some other models the surface diffusivity is assumed to be proportional (PD) to the particle radius or a complex function of it. For example, Badruzzaman[25] found that the adsorption of arsenate over granular ferric hydroxide (GFH) could be correlated with the equation $D_s = 3\times10^{-9}\ R_p{}^{1.4}$. Such dependence is disregarded here and a 'constant diffusivity' (CD) approach is used.

Internal particle diffusion involves both pore and surface diffusion. It is difficult to separate these two mechanisms because

Table 2. Description of symbols in Equations (1)–(10). Numerical values corresponding to the experimental breakthrough test (RSSCT) and the simulation of the industrial packed bed adsorber

Symbol	Value		Description and units
	Laboratory RSSCT	Industrial packed bed	
ε_B	0.45	0.45	Bed porosity, dimensionless
ε_p	0.557	0.56	Pellet porosity, dimensionless
ε	0.756	0.756	Total porosity, dimensionless
ρ_s	2.1	2.1	Solid density, g cm^{-3}
ρ_p	0.929	0.929	Particle density, g cm^{-3}
R_p	0.17 (35x80)	0.53 (12x40)	Particle radius, mm (mesh)
d_t	0.9	74	Tube (bed) diameter, cm
L	25	224	Bed length, cm
L/d_t	28	3	Height-to-diameter ratio
F	18.5	(10.4)	Flowrate, mL min^{-1} (m^3 h^{-1})
W	11	(500)	Adsorbent mass, g (kg)
V_B	23	(0.98)	Bed volume, cm^3 (m^3)
U	4.9	6.6	Empty reactor velocity, $U = \varepsilon u$, mm seg^{-1}
u	10.8	–	Insterticial velocity, u, mm seg^{-1}
EBCT	0.86	5.6	Empty bed contact time, min
D_M	4.4×10^{-10}	–	Molecular diffusivity of arsenate in water, m^2 s^{-1}
D_s	2.0×10^{-13}	2.0×10^{-13}	Surface diffusivity of arsenic, 25 °C, m^2 s^{-1}
H	21.8	21.8	Henry's constant for adsorption, L g_{ads}^{-1}
μ	1.0	–	Viscosity of the water solution, cp
P	1.0	–	Density of the water solution, g cm^{-3}
Sc	2270	–	$\mu/(\rho D_m)$, Schmidt number, dimensionless
Re	3.7	–	$u\rho D_s/\mu$, Reynolds number, dimensionless
D_L	1.8×10^{-6}	–	Axial diffusivity, m^2 s^{-1}, calculated with Eq. (6)
Sh	33.5	–	$2R_p k_f/D_M$, Sherwood number, dimensionless
Pe	658	–	UL/D_L, Axial Pèclet number, dimensionless
Bi	1.8	–	$k_f R_p/H\rho_p D_s$, Biot number, dimensionless
k_f	4.3×10^{-5}	–	Film mass transfer coefficient, m s^{-1}
q_m	1850	–	Saturation adsorption capacity, μg_{As} g_{ads}^{-1}
K	0.0075	–	Langmuir constant, L^{-1} μg_{As}
C^0	100	100	Feedstock arsenic concentration, μg_{As} L^{-1}

the models produce fits of similar quality. For organic compounds adsorbed by activated carbon, surface diffusion is dominant by almost a factor of 20 over pore diffusion.[26] Calculations of D_M for arsenate with the Wilke–Chang equation and D_s from the fit of experimental data with Equation (12) indicates that $D_s/D_M \approx 10^2$–10^4. Axe and Trivedi[27] studied a long series of inorganic oxides and concluded that intraparticle surface diffusion is the rate limiting process for metal ion adsorption by microporous metal oxides in water environments.

The model thus written can be solved with its full complexity or some simplifying assumptions can be made. First, the non-linearity of the equilibrium adsorption isotherm formula can be removed by adopting the square isotherm or the linear isotherm models. The first option is taken for adsorption systems in which the surface has a high affinity for the adsorbate over the whole concentration range. Teo and Ruthven[28] used it to simulate the adsorption of water from ethanol solutions onto 3A zeolites. All reports use the formulae first derived by Weber and Chakravorti[29] for a system constrained by both pore and film diffusion. These formulae are not valid in our case because most groundwaters contain As^V in concentration values between 10 and 200 μg_{As}^{-1} L. The linear isotherm can be applied in this range.

The Langmuir isotherm formula (Equation (1)) can then be replaced by $q = HC_{As}$, where q is the equilibrium adsorbate load and H is Henry's constant for adsorption. Also in Equation (8) C_s should be replaced by (q_s/H). The modified set of equations can now be solved and an analytical set of expressions for the solution can be written. These formulae have been previously derived by Rasmuson and Neretnieks[30] and Xiu *et al.*[31]

The exact solution is complex because it involves the resolution of an integral. Some approximate solutions are usually used instead. Two of these solutions are the 'parabolic profile' and the 'quasi-log normal distribution' (Q-LND).[32] In the first case the profile of the concentration of the adsorbate in the adsorbent is assumed to be parabolic. The set of equations in this case is simpler but also of algebraic-integral nature. In the second case[33] it is assumed that the quasi-lognormal probability density function, $y_\delta(\tau)$, can be used to represent the impulse response of the system, where $y_\delta(\tau)$ is the product of the lognormal probability density function and the zeroth moment of the impulse response of the system, μ_0:

$$y_\delta(\tau) = \frac{\mu_0}{\sqrt{2\pi}\sigma\tau} \exp\left[-\frac{(\ln\tau - \mu)^2}{2\sigma^2}\right] \qquad (14)$$

The approximation of a step response, i.e. the breakthrough curve, $y_B(\tau)$, is simply the integral of the impulse response, and it has been reduced in Equation (15) to a 'compact' form using the error function.

$$y_B(\tau) = \int_0^\tau y_\delta(\tau)d\tau = \frac{1}{2}\mu^o\left(1 + erf\left\{\frac{(\ln(\tau) - \mu)}{(\sigma\sqrt{2})}\right\}\right) \quad (15)$$

where y is the adimensional adsorbate concentration and τ is the adimensional time. The μ and σ parameters are algebraic functions of the Péclet number (*Pe*), the modified Biot number (*Bi*) and the time parameter (θ, ratio of space time and intraparticle diffusion time).

$$Bi = \frac{k_f R_p}{HD_s\rho_s} \quad (16)$$

$$Pe = \frac{uL}{\varepsilon_B D_L} \quad (17)$$

$$\theta = \frac{\varepsilon_B L D_s}{uR_p^2} \quad (18)$$

$$y = \frac{C}{C^o} \quad (19)$$

$$\tau = \frac{t}{D_s R_p^2} \quad (20)$$

$$\zeta = \frac{z}{L} \quad (21)$$

$$\mu = \ln\mu_1 - \frac{1}{2}\ln(1 + \frac{\mu'_2}{\mu_1^2}) \quad (22)$$

$$\sigma = \left[\ln(1 + \frac{\mu'_2}{\mu_1^2})\right]^{1/2} \quad (23)$$

$$\mu_0 = 1 \quad (24)$$

$$\mu_1 = \zeta\theta[1 + \delta_m] \quad (25)$$

$$\mu'_2 = \frac{2}{3}\zeta\theta\delta_m\left(\frac{1}{5} + \frac{1}{Bi}\right) + \frac{2\zeta\theta^2}{Pe}[1 + \delta_m]^2 \quad (26)$$

$$\delta_m = \left(\frac{1 - \varepsilon_B}{\varepsilon_B}\right)H\rho_s \quad (27)$$

It has been demonstrated that the analytical solution and the approximate solutions are similar for a wide range of the model parameters. Deviations in both approximations (parabolic profile and Q-LND) occur for very low values of the residence time.[33]

Experimental and simulated breakthrough curves

Estimations can first be made to calculate both the film and intrapellet mass transfer resistances. The molecular diffusivity, D_M, of arsenate in water and its superficial diffusivity in porous media (D_s) have been measured by many researchers. A value of D_M of 4.4×10^{-10} m^2 s^{-1} and an approximate value of D_s of 2.0×10^{-13} m^2 s^{-1} can be taken from these references.[15,21,34] The value of D_M can be used to calculate the film resistance with Equation (7) ($k_f = 1.6 \times 10^{-5}$ m s^{-1}). R_p is equal to 0.2 mm. The calculation of the individual resistances indicates that the intrapellet diffusion is the biggest mass transfer resistance.

$$film\ resistance = 1/k_f = 6.2 \times 10^4\ \text{s cm}^{-1}$$

$$intrapellet\ resistance = R_p/4\,\varepsilon_p\,D_s = 4.4 \times 10^8\ \text{s cm}^{-1}$$

The value of D_s could be further refined by fitting the model to the experimental data with an optimization algorithm. A value of about 9×10^{-14} m^2 s^{-1} was found. Figure 2 shows the results of the breakthrough test. A theoretical curve based on the Q-LND approximate solution is also plotted. The value of H was found from the experimental curve and an equation derived from Equations (2) and (4):

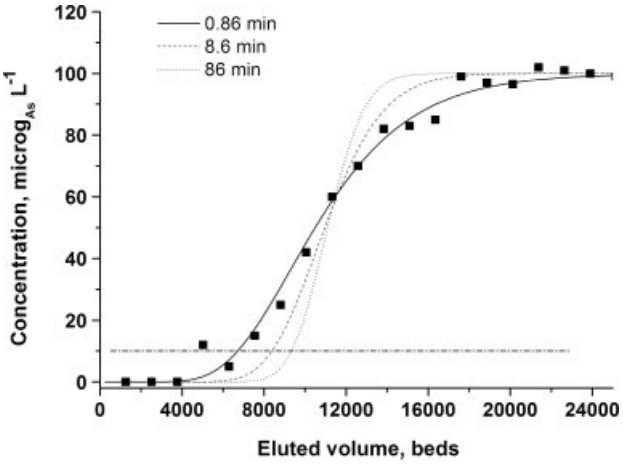

Figure 2. Influence of empty bed contact time (*EBCT*) on the adsorbent performance. Experimental (■) (*EBCT* = 0.86 min) and theoretical breakthrough curves for a feedstock with an As concentration of 100 μg L^{-1} and three different flowrates. Dash-dotted line: OMS 10 μg$_{As}$ L^{-1} limit.

$$H = \frac{\int_0^\infty (C^o - C)dV}{C^o W_{ads}} \quad (28)$$

The calculated H value is 21.8 L g$_{ads}^{-1}$.

This is quite different from the value of 8.51 g$_{ads}^{-1}$ L taken from the equilibrium adsorption test, indicating that the validity of the equilibrium experimental data has been hampered by the high value of the intraparticle mass transfer resistance. In Fig. 2, the theoretical curve was plotted using the above calculated H, D_M and k_f parameters.

As can be seen, the match between the experimental and theoretical breakthrough curve is fairly good. At the conditions chosen the outlet concentration value of 10 μg$_{As}$ L^{-1} is obtained for an eluted volume of 6000 bed volumes kg$_{ads}^{-1}$. Now new curves can be obtained by using the same H value and the same mass transfer parameters.

Two more curves were plotted varying the flowrate. It can be seen that the efficiency of the packed adsorbent is increased when the spatial velocity is decreased. When the spatial velocity goes to zero the breakthrough curve should be a step function. The eluted volume for 100% filter efficiency corresponds to the point of intersection of all the curves of varying space velocity, i.e. about 8.8 m^3 kg$_{ads}^{-1}$. Therefore at the conditions of the experimental test the breakthrough point is achieved when only 61% of the adsorption capacity of the filter is used. It seems clear that the spatial velocity should be reduced as much as possible; this cannot be done arbitrarily. The required throughput of purified water is normally fixed and too small a spatial velocity would lead to small residence times and big reactor volumes. One intermediate solution to the problem is to avoid high flowrates during peaks of demand by introducing a sufficiently big buffer tank. Then the adsorption column can be operated without idle times at the minimum possible flowrate.

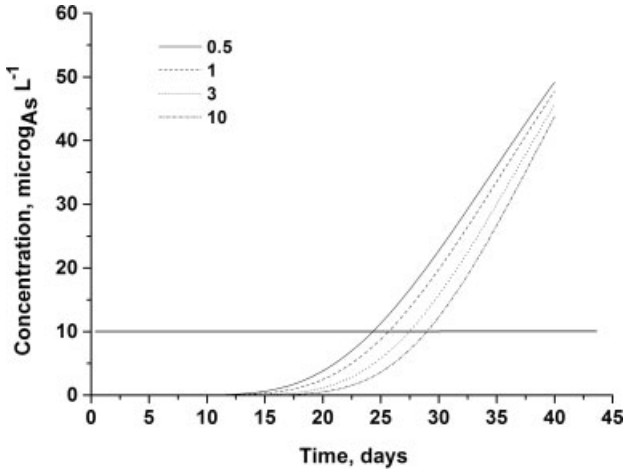

Figure 3. Simulated breakthrough curves of an industrial packed bed adsorber. Influence of height-to-diameter ratio at constant flowrate, adsorbent mass and residence time. See Table 2 for values of process conditions.

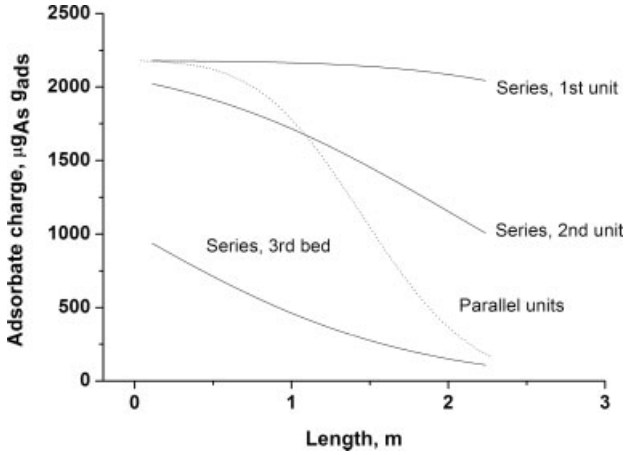

Figure 4. Surface concentration of adsorbate as a function of the position along the bed at the time of the breakthrough (10 μg_{As} L^{-1} limit). Comparison between parallel and series arrangements of three industrial packed bed adsorbers.

Figure 2 also shows that the dependence of the breakthrough point on the spatial velocity is highly non-linear. When the velocity is reduced ten times (from 0.46 to 0.046 mm s^{-1}) the breakthrough point is increased only by 18% (from 5.4 to 6.4 m^3 $kg_{ads}{}^{-1}$). This is related to the rather asymptotic pattern of saturation of porous pellets with diffusion limitations. The more saturated the pellet is the more difficult it is to continue saturating.

Figure 3 shows simulation results for the approximate model of an industrial packed bed. The dimensions and process conditions are indicated in Table 1. Figure 3 contains breakthrough curves for different geometries of adsorber (different length-to-diameter ratio) but with same adsorbent mass and water feed flowrate. It can be deduced that for the three curves the EBCT (empty bed constant time) is the same. It can be seen that at constant residence time the efficiency of the Fe/GAC filter is increased by using higher *L/D* ratios. In this case part of the effect can be attributed to the decrease of mass transfer resistance in the film surrounding the particles at higher Re values. Considering that k_f, the film mass transfer coefficient, is a function of the length-to-diameter ratio: $k_f(0.5) = 1.037 \times 10^{-5}$; $k_f(1.0) = 1.34 \times 10^{-5}$; $k_f(3) = 2.04 \times 10^{-5}$; $k_f(10) = 3.25 \times 10^{-5}$ (in m s^{-1} units). The use of filters with high *L/D* ratio is only discouraged by the complexity of the equipment, which needs to use multiple supporting trays to avoid crushing the particles in the bottom.

An alternative solution is the use of filters in series, but there exists a trade-off with the increased cost in piping and manifolds. In any case, a simulation was performed to see the difference in breakthrough time for a limit of 10 $\mu g\ L^{-1}$ when using three adsorbers in series and three adsorbers in parallel for processing three times the flowrate (industrial adsorber, conditions in Table 2). The parallel combination of adsorbers can be used for 27.5 days while the series arrangement can be used for 29.4 days. Thus the efficiency is higher for the series pattern although there is a trade-off and this is the increased pressure drop.

Another advantage of the series arrangement is that of adsorbent disposal and replacement. In the parallel arrangement all units achieve the breakthrough point at the same point and therefore all must be replaced. In the case of the series arrangement the upstream units are more saturated than the downstream ones, and only these should be replaced. Downstream units can be kept

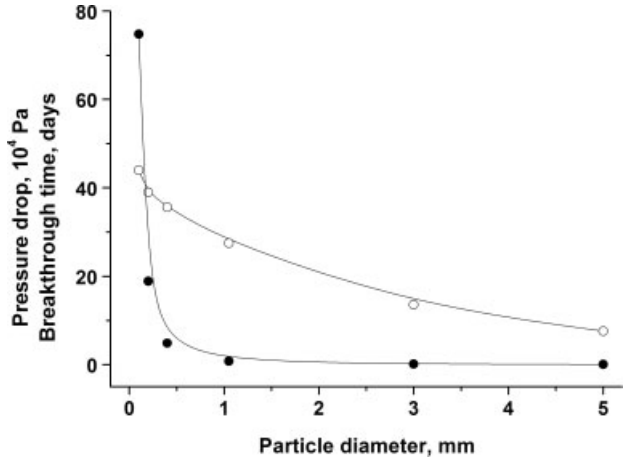

Figure 5. Influence of the particle radius on time of breakthrough (10 μg_{As} L^{-1} limit) and on the pressure drop in an industrial packed bed adsorber. (●) Pressure drop; (○) breakthrough time.

and for an optimal replacement sequence the fresh adsorbent unit should be placed downstream from the older ones. For example, the profiles of Fig. 4 clearly indicate that the first two units in the series arrangement are completely saturated while the last unit is only half saturated. In the case of the parallel arrangement all are saturated to about 80%.

Figure 5 contains plots of the pressure drop and the time of breakthrough for the industrial packed bed adsorber. The pressure drop was calculated using Ergun's correlation:

$$\Delta P = \frac{L\rho U^2}{2R_p}\left(\frac{1-\varepsilon_B}{\varepsilon_B^3}\right)\left(1.75 + \frac{150\mu(1-\varepsilon_B)}{2R_pU\rho}\right) \qquad (29)$$

The results indicate that pressure drop becomes excessive for particle diameters smaller than 0.5 mm while breakthrough times become too small for particle diameters greater than 2 mm.

At this point it seems convenient to simulate packed beds of smaller size, especifically, those used in point-of-use domestic filters. These devices have the big drawback of using extremely small EBCT values, such as those needed to fill a glass with water.

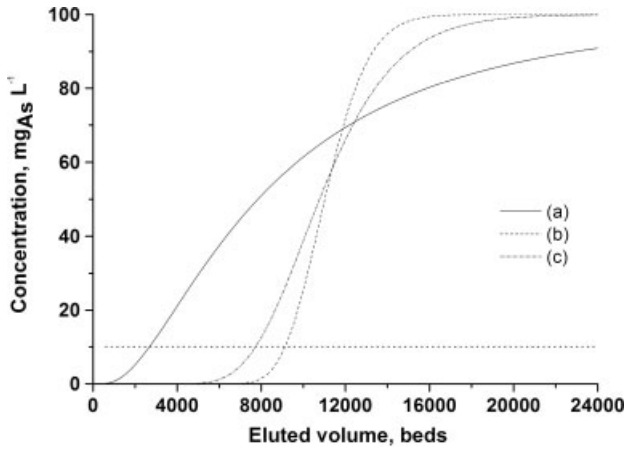

Figure 6. Influence of residence time (*EBCT*) and particle size on the performance of point-of-use home filters packed with Fe/GAC adsorber. Simulated breakthrough curves. Filter volume = 1.3 L, $C^o = 100\ \mu g_{As}\ L^{-1}$, $Q^* = 11000$ beds. (a) 10 s EBCT, 20 × 40 mesh. (b) 1000 s EBCT, 20 × 40 mesh. (c) 10 s EBCT, 100 × 140 mesh.

Figure 6 contains breakthrough curves of a small filter fed with water with 100 $\mu g_{As}\ L^{-1}$ for different EBCTs and particle sizes. As can be seen, for a normal EBCT of 10 s and a particle size of 20 × 40 the outlet concentration reaches the value of 10 $\mu g\ L^{-1}$ when only 20% of the filter has been used. In order to increase the filter use, if the particle size is not changed, completely unattainably high values of EBCT must be used, e.g. 10^3 s.

These diffusion problems for drinking tap devices can be solved by using mesopore instead of microporous carbons. Gu *et al.*[18] used ordered mesoporous carbons, impregnated with iron with a 4 nm average pore size, and found that arsenate removal is effective while mass transfer restrictions are much reduced. A simpler solution could be the reduction of the carbon particle size. Figure 6(c) indicates that for a EBCT of 10 s, using a particle size of 100 × 200 mesh increases filter usage to 50% at the 10 $\mu g\ L^{-1}$ limit. To use such small particle sizes either higher pressure drops must be tolerated or filters with cylindrical geometries and radial flow must be used.

CONCLUSIONS

An analysis of the results of this work enables us to draw the following conclusions: (i) The adsorption isotherm of As^V on Fe/GAC adsorbents can be taken as approximately linear in the 0–300 $\mu g_{As}\ L^{-1}$ range, a common range for the groundwaters of the Argentine Central Plains and other world aquifers. (ii) Adopting the linear isotherm and assuming intrapellet homogeneous surface diffusion with constant diffusivity, a model for flow and adsorption of As inside packed bed adsorbers can be written and conveniently solved and reduced to an analytic compact solution using the quasi-lognormal distribution approximation. (iii) The use of this approximate model for the simulation of industrial adsorbers and point-of-use home filters indicates that both systems are constrained by the low surface diffusivity of As, but that the performance is especially low in home filters due to very short contact times. For these home filters particle reduction would increase the filter efficiency but this is prevented by pressure drop considerations. (iv) For industrial adsorbers with big particle sizes the model also predicts incomplete adsorbent usage at the breakthrough condition, but a relatively high efficiency can be obtained in this case owing to much smaller contact times and the possibility of improved operation (use of buffer tanks, countercurrent flow pattern, etc.).

ACKNOWLEDGEMENTS

The authors gratefully acknowledge the financial support of Universidad Nacional del Litoral (Grant PI 36-199) and CONICET (Argentina).

REFERENCES

1 WHO, *Environmental Health Criteria 224: Arsenic compounds* 2nd edn. World Health Organisation, Geneva (2001).
2 Farías S, Casa V, Vázquez C, Ferpozzi L, Pucci G and Cohen I, Natural contamination with arsenic and other trace elements in ground waters of Argentine Pampean Plain. *Sci Total Environ* **309**:187–199 (2004).
3 Smedley PL, Kiniburgh DG, Huq I, Zhen-Dong L and Nicolli HB, International perspective on naturally occuring arsenic problems in groundwater. *Proceedings of the 4th International Conference on Arsenic Exposure and Health Effects,* June 18–22, (2000). San Diego, CA, USA, pp. 9–25.
4 Sigrist M, Albertengo A, Beldoménico H and Tudino M, Determination of As(III) and total inorganic As in waters amples using an on-line solid phase extraction and flow injection hydride generation atomic absorption spectrometry. *J Hazard Mater* **188**:311–318 (2011).
5 Choong TSY, Chuah TG, Robiah Y, Gregory Koay FL and Azni I, Arsenic toxicity, health hazards and removal techniques from water: an overview. *Desalination* **217**:139–166 (2007).
6 US EPA, *Arsenic Treatment Technology Evaluation Handbook for Small Systems.* EPA 816-R-03-014, July (2003).
7 Porter MC (ed), *Handbook of Industrial Membrane Technology*. Noyes Publications (1990).
8 Westerhoff P, Karanfil T and Crittenden J, Aerogel and iron-oxide impregnated granular activated carbon media for arsenic removal. Final Report, AWWA Research Foundation (2006).
9 Sperlich A, Werner A, Genza A, Amy G, Worch E and Jekel M, Breakthrough behavior of granular ferric hydroxide (GFH) fixed-bed adsorption filters: modeling and experimental approaches. *Water Res* **39**:1190–1198 (2005).
10 Westerhoff P, Highfield D, Badruzzaman N and Yoon Y, Rapid small-scale column tests for arsenate removal in iron oxide packed bed columns. *J Environ Eng* **131**:262–271 (2005).
11 Badruzzaman M, Mass transport scaling and the role of silica on arsenic adsorption onto porous iron oxide (hydroxide). PhD Thesis, Arizona State University, December (2005).
12 Solozhenkin PM, Deliyanni EA, Bakoyannakis VN, Zouboulis AI and Matis KA, Removal of As(V) ions from solution by akaganeite *bgr*-FeO(OH) nanocrystals. *J Mining Sci* **39**:287–296 (2003).
13 Parsons JG, Lopez ML, Peralta-Videa JR and Gardea-Torresdey JL, Determination of arsenic(III) and arsenic(V) binding to microwave assisted hydrothermal synthetically prepared Fe_3O_4, Mn_3O_4, and $MnFe_2O_4$ nanoadsorbents. *Microchem J* **91**:100–106 (2009).
14 Gu Z, Fang J and Deng B, Preparation and evaluation of GAC-based iron-containing adsorbents for arsenic removal. *Environ Sci Technol* **39**:3833–3843 (2005).
15 Chen W, Parette R, Zou J, Cannon FS and Dempsey BA, Arsenic removal by iron-modified activated carbon. *Water Res* **41**:1851–1858 (2007).
16 Sato S, Yoshihara K, Moriyama K, Machida M and Tatsumoto H, Influence of activated carbon surface acidity on adsorption of heavy metal ions and aromatics from aqueous solution. *Appl Surf Sci* **20**:8554–8559 (2007).
17 Hijnen WA, Suylen GM, Bahlman JA, Brouwer-Hanzens A and Medema GJ, GAC adsorption filters as barriers for viruses, bacteria and protozoan (oo)cysts in water treatment. *Water Res* **44**:1224–1234 (2010).
18 Gu Z, Deng B and Yang J, Synthesis and evaluation of iron-containing ordered mesoporous carbon (FeOMC) for arsenic adsorption. *Micropor Mesopor Mater* **102**:265–273 (2007).
19 Hristovski KD, Westerhoff PK, Möllerc T and Sylvester P, Effect of synthesis conditions on nano-iron (hydr)oxide impregnated granulated activated carbon. *Chem Eng J* **146**:237–243 (2009).

20 Ruthven DM, *Principles of Adsorption and Adsorption Processes*. John Wiley & Sons Inc., New York (1984).
21 Ouvrard S, Simonnot MO, de Donato P and Sardin M, Diffusion-controlled adsorption of arsenate on a natural manganese oxide. *Ind Eng Chem Res* **41**:6194–6199 (2002).
22 Carberry JJ, *Chemical and Catalytic Reaction Engineering*. Mc-Graw Hill, New York (1976).
23 Moate JR and LeVan MD, Fixed-bed adsorption with nonplug flow: perturbation solution for constant pattern behavior. *Chem Eng Sci* **64**:1178–1184 (2009).
24 Vaughan Jr. RL, Reed BE and Smith EH, Modeling As(V) removal in iron oxide impregnated activated carbon columns. *J Environ Eng* **133**:121–124 (2007).
25 Badruzzaman M, Westerhoff P and Knappe DR, Interparticle diffusion and adsorption of arsenate onto granular ferric hydroxide (GFH). *Water Res* **38**:4002–4012 (2004).
26 Komiyama H and Smith JM, Surface diffusion in liquid-filled pores. *AIChE J* **20**:1110–1117 (1974).
27 Axe L and Trivedi P, Intraparticle surface diffusion of metal contaminants and their attenuation in microporous amorphous Al, Fe, and Mn Oxides. *J Colloid Interf Sci* **247**:259–265 (2002).
28 Teo WK and Ruthven DM, Adsorption of water from aqueous ethanol using 3-A molecular sieves. *Ind Eng Chem Process Des Dev* **25**:17–21 (1986).
29 Weber TW and Chakravorti RK, Pore and solid diffusion models for fixed-bed adsorbers. *AIChE J* **20**:228–237 (1974).
30 Rasmuson A and Neretnieks I, Exact solution of a model for diffusion in particles and longitudinal dispersion in packed beds. *AIChE J* **26**:686–690 (1980).
31 Xiu GH, Modeling breakthrough curves in a fixed bed of activated fiber. Exact solution and parabolic approximation. *Chem Eng Sci* **51**:4039–4041 (1996).
32 Li P, Xiu G and Rodrigues AE, Modeling breakthrough and elution curves in fixed beds of inert core adsorbents: analytical and approximate solutions. *Chem Eng Sci* **59**:3091–3103 (2004).
33 Xiu GH, Nitta T, Li P and Jin G, Breakthrough curves for fixed-bed adsorbers: quasi-lognormal distribution approximation. *AIChE J* **43**:979–985 (1997).
34 Raven KP, Jain A and Loeppert RH, Arsenite and arsenate adsorption on ferrihydrite: kinetics, equilibrium, and adsorption envelopes. *Environ Sci Technol* **32**:344–349 (1998).

